Supporting Information

A joint DFT-kMC study to model ethylene carbonate decomposition reactions: SEI formation, growth, and capacity loss during calendar aging of Li-metal batteries

Mohammed Bin Jassar,[1,2,3] Carine Michel,[2] Sara Abada,[4] Theodorus De Bruin,[3] Sylvain Tant,[1] Carlos Nieto-Draghi,[3] and Stephan N. Steinmann[2*]*

[1]Stellantis - Centre Technique de Carrière-sous-Poissy, 212 Boulevard Pelletier78955 Carrière-sous-Poissy, France

[2]ENS de Lyon, CNRS, Laboratoire de Chimie UMR 5182, 69364 Lyon, France

[3]IFP Energies nouvelles, 1 et 4 venue de Bois-Préau, 92852 Rueil-Malmaison, France

[4]IFP Energies nouvelles, Rond-Point de l'échangeur de Solaize, BP 3, 69360 Solaize, France

Corresponding Authors

* E-mail: carlos.nieto@ifpen.fr; stephan.steinmann@ens-lyon.fr

Table of Contents

1. DFT

1.1 DFT Additional Results

Figure S1 : Surfaces used in our calculations Li_2CO_3 (001) and Li_2O (111). Li: green, O: red, C: brown.

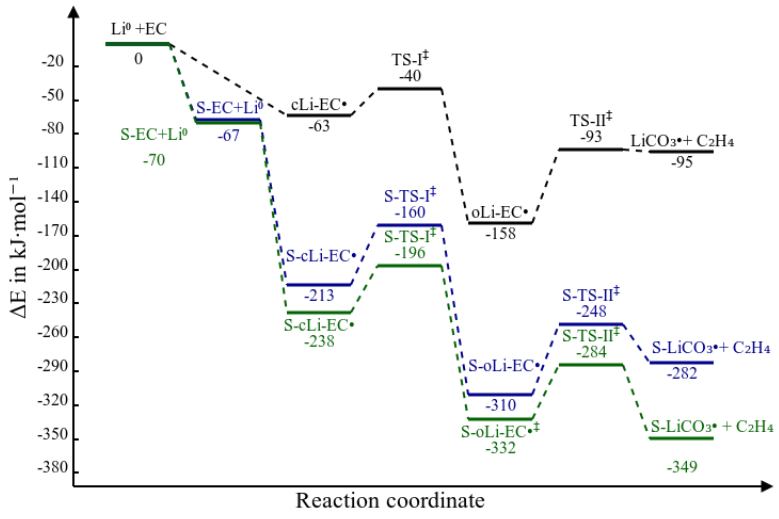

Figure S2: EC decomposition reactions, in isolation (black), over Li_2CO_3 (001) (blue) and over Li_2O (111) (green), S stands for surface

Carrying reactions over Li_2O (111) led to a different behavior compared to the case in isolation and over Li_2CO_3 (001), see Figure S2. The geometries of species over Li_2CO_3 (001) and Li_2O (111) are shown in Figure S3 and Figure S4 respectively. Table S1 shows all energy barriers and reaction energies included in our study. It should be noted that the high barrier for Li_2BDC

formation over Li_2O (111) could be explained by the relative stability of oLi-EC• over Li_2O (111) with respect to the cases in isolation and over Li_2CO_3 (001): one of the two oLi-EC• reactants forming Li_2BDC is connected to Li_2O (111) with all the three oxygen atoms, see Figure S4e, making it hard to form through the C-C coupling reaction. Table S2 shows the length of bonds broken/formed for the obtained TS geometries.

Table S1: Reaction energies (E_r), energy barriers for the forward (E_b) and backward (E_{bb}) reactions in kJ/mol

Reaction	**in isolation**			**over Li_2CO_3 (001)**			**over Li_2O (111)**		
	E_b	E_r	E_{bb}	E_b	E_r	E_{bb}	E_b	E_r	E_{bb}
I	23	-95	118	53	-97	150	42	-94	126
II	65	63	2	62	29	34	48	-17	65
III	0	-375	375	0	-362	362	0	-356	356
IV	0	-383	383	13	-361	374	53	-365	418
V	0	-322	322	0	-232	232	0	-224	224
VI	0	-437	437	0	-391	391	0	-339	339

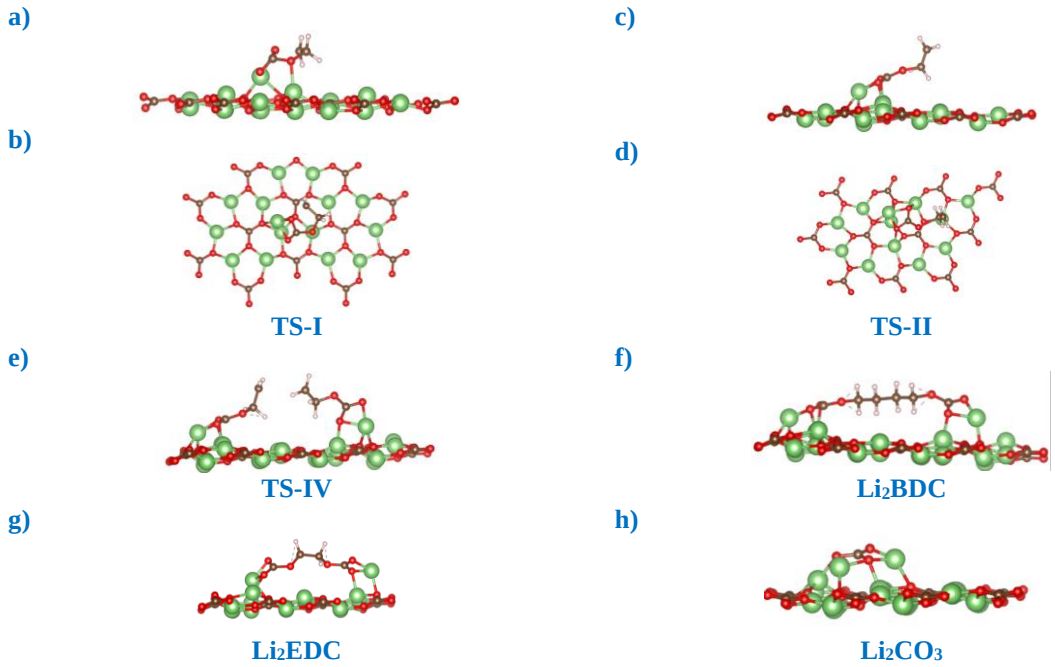

Figure S3: EC decomposition reactions over Li_2CO_3 (001): a and b are side and top views of transition state geometry of RI respectively. c and d are side and top views of transition state geometry of RII respectively. e-h) Structures of TS-RVI, Li_2BDC and Li_2EDC and Li_2CO_3

respectively. Only top layer of the surface in contact with reactive species is shown. Li: green, O: red, C: brown, H: gray.

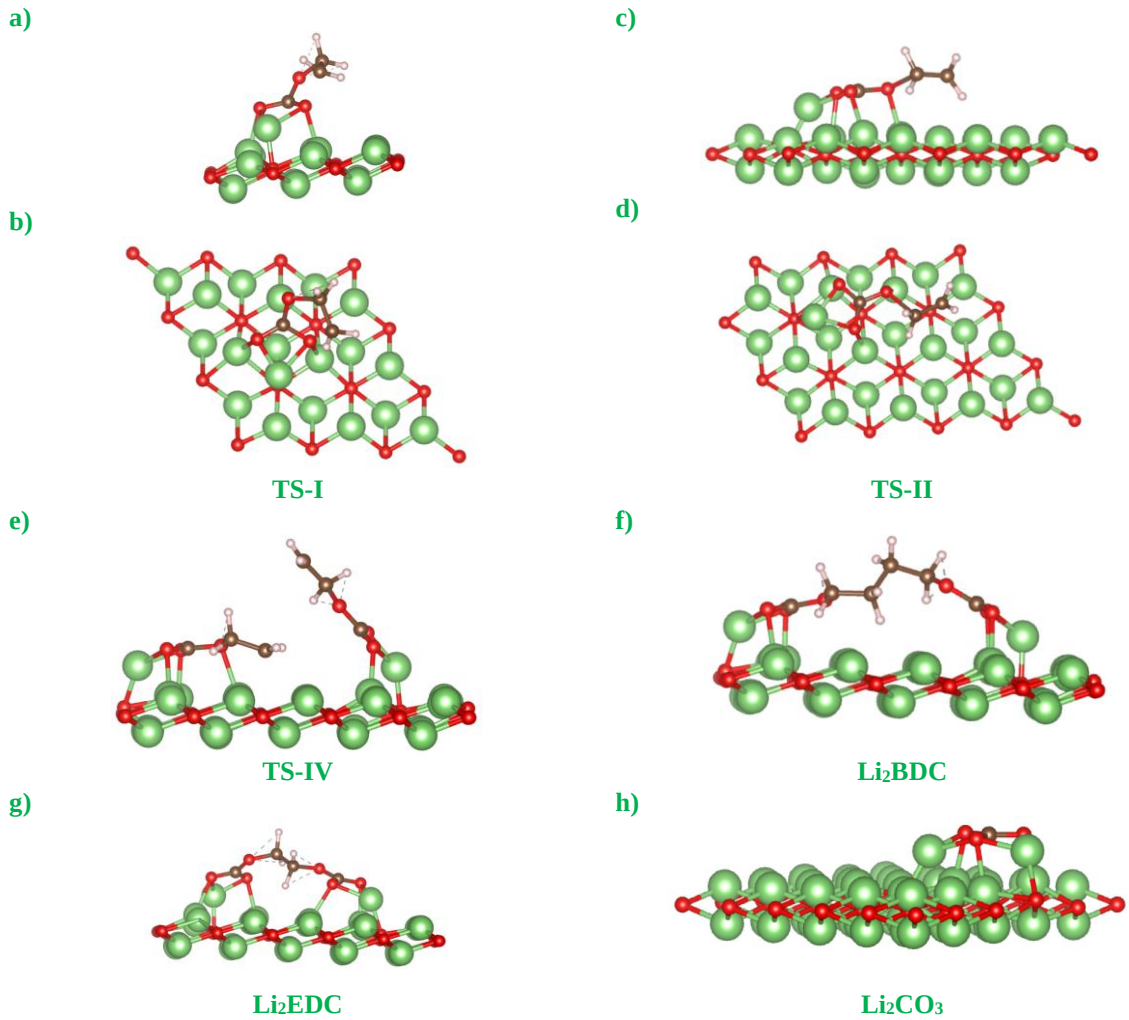

Figure S4: EC decomposition reactions over Li_2O (111): a and b are side and top views of transition state geometry of RI respectively. c and d are side and top views of transition state geometry of RII respectively. e-h) Structure of TS-RVI, Li_2BDC and Li_2EDC and Li_2CO_3 respectively. Only top layer of the surface in contact with reactive species is shown. Li: green, O: red, C: brown, H: gray.

Table S2: The length of bonds broken/formed for transition state (TS) geometries (in Å)

TS	In Isolation	Over Li_2CO_3 (001)	Over Li_2O (111)
I	1.68	1.73	1.70
II	2.30	2.16	1.90
IV	##	3.48	4.00

1.2 Typical INCAR file for DFT Calculations

PREC = Accurate	Specifies the "precision"-mode
ALGO = Fast	Selects a robust mixture of the Davidson and RMM-DIIS algorithms
ENCUT = 600	Specifies the cutoff energy for the plane-wave-basis set in eV.
ISMEAR= -1	Fermi smearing: good for semiconductors and molecules
SIGMA= 0.03	Width of the smearing in eV.
GGA = PE	Specifies the exchange-correlation functional Perdew-Burke-Ernzerhof
EDIFF=10E-6	Global break condition for the electronic SCF-loop
LREAL=Auto	Fully automatic optimization of projection operators
MAXMIX = 20	Specifies the maximum number steps stored in Broyden mixer
LCHARG =.F.	No CHGCAR file written
LWAVE =.F.	No WAVECAR file written
NSW = 100	Maximum number of ionic steps
IBRION = 2	Ionic relaxation (conjugate gradient algorithm)
EDIFFG=-0.03	Break condition for the ionic relaxation loop: Maximum gradient (eV/A)
ISPIN=2 #	Spin polarized calculations (collinear) are performed
MAGMOM=1*0 3*0 2*0 1 4*0	Specifies the initial magnetic moment for each atom
NUPDOWN=1	Difference between alpha and beta electrons
LORBIT=14	Better output regarding the spin population
IVDW=4 #	Dispersion correction

2. Kinetic Monet Carlo (kMC)

In kMC, the evolution of chemical reactions in function of time can be expressed by means of a Master Equation[1]:

$$\frac{dP_\alpha}{dt} = \sum_\beta [W_{\alpha\beta}P_\beta - W_{\beta\alpha}P_\alpha] \qquad (S1)$$

where t is time, α and β are configurations, $P_\propto$ and P_β are their probability. $W_{\alpha\beta}$ and $W_{\beta\alpha}$ are transition probabilities per unit time that specify the rate of changes due to reactions. The transition probabilities can be obtained with quantum chemical methods[2]. The first term on the right side of the Eq. (S1) stands for the increase in P_α when other configuration changes to α; the second term is for the reaction of α. kMC replaces reaction probabilities by rate constants

and assumes that the probability distribution $P_{rx}(t)$ of the time (t) that a reaction occurs is a Poisson process[1], i.e., it is given by:

$$P_{rx}(t) = k\, e^{-k(t-t_{now})} \qquad (S2)$$

, where k is the rate constant and t_{now} is the current time. The rate constant can be obtained from the transition state theory (TST) according to Eq. (S3)[2]:

$$k = \frac{k_B T}{h} \frac{q^{\ddagger}}{q} \exp\left[-\frac{E_b}{k_B T}\right] \qquad (S3)$$

, where E_b is the energy barrier obtained from our DFT calculations, k_B is the Boltzmann constant, T is the absolute temperature, h is Planck's constant and $\frac{q^{\ddagger}}{q}$ is the ratio of the partition function between the initial and the transition state. This ratio is generally considered almost unity, assuming the situation where the entropy of the transition state of a reaction does not differ from the one of the reactants. Hence, we only have $\frac{k_B T}{h}$ which, in our simulation, is approximated to $k_0 = 10^{13}$ s^{-1} [2–4]. Consequently, the simpler form of the rate constant equation is:

$$k = k_o \exp\left[-\frac{E_b}{k_B T}\right] \qquad (S4)$$

where k_0 is the pre-exponential factor.

The principle of kMC is to start with a particular configuration and then predict the subsequent configurations. If a system is at configuration α, then the probability that the system stays at the same configuration is given by:

$$Q_{\alpha\alpha}(t) = \exp(-R_{\alpha\alpha}t) \quad (S5)$$

, where Q is the matrix of probabilities and R is the diagonal matrix of reactions. The probability distribution for the system to stay at the same configuration (first reaction) at time t' is given by:

$$r_1 = \exp(-R_{\alpha\alpha}t') \quad (S6)$$

, where r_1 a random number $\in [0,1)$. However, for a reaction to go from a configuration α to a configuration β, it should occur following $W_{\beta\alpha}$ generating a new configuration α' at time t' from all possible new configuration β with a probability proportional to $W_{\alpha'\alpha}$. The algorithm continues (if the end time of simulation has not reached yet) to go to the next step and increase the time to t'' according to the following equation:

$$r_2 = \exp(-R_{\alpha'\alpha'}(t'' - t')) \quad (S7)$$

The state of the system in kMC evolves by randomly selecting an event (diffusion or reaction) and its corresponding rate constant through:

$$\sum_{i=0}^{k-1} N_i k_i \; < \; \rho_1 \sum_i N_i k_i \leq \sum_{i=0}^{k1} N_i k_i \quad (S8)$$

where N_i is the number of reactions type i, k_i is the rate constant of reaction i, $\sum_i N_i k_i$ is the total rate and ρ_1 is a random number $\in [0,1)$.

What makes kMC different than other Monte Carlo methods is the "notion" of time. In regular MCs, there is no time evolution, only sampling an equilibrium distribution. The time in kMC is increasing deterministically and is drawn from a Poissonian distribution[1]:

$$\Delta t = \frac{\ln(\rho_2)}{\sum_i N_i k_i} \quad \text{(S9)}$$

where Δt is the time elapsed between two consecutive events occurring in the system and ρ_2 is a random number $\in [0,1)$. In addition, kMC method allows a spatial resolution of the system with local concentration of species[1]. Additional and more details about the kMC methodology are found in the literature[1,5–7].

2.1 Link between diffusion rate constants and diffusion coefficients through the Mean Square Displacement (MSD) in kMC simulations

SPPARKS software allows for calculating of diffusion coefficients D of species where specie (e.g., vacant site) can be swapped by another diffusing species (jump from one site to the other), see Eq. (S10) and Eq. (S11):

$$X + \text{vacant site} \rightarrow \text{vacant site} + X \quad \text{(S10)}$$

$$D = \frac{1}{2 \times ddl} \times \nu \times \Delta d^2 \quad \text{(S11)}$$

where ddl is the degree of freedom (ddl = 3 in 3D), ν is the diffusion rates (s^{-1}) and Δd is the average distance between sites (3.8 Å in our system). To extract the diffusion coefficient from the trajectories of a particle, the mean square displacement (MSD) method was used. For a particle i:

$$MSD_i = \left| d_{i,t} - d_{i,t_0} \right|^2 \quad \text{(S12)}$$

, where $d_{i,t}$ is the position of the molecule i at time t and d_{i,t_0} is the position at time t_0. The diffusion coefficient D is related to MSD through:

$$D = \frac{MSD}{t} \qquad (S13)$$

So, we can obtain D from the slope of the linear curve of MSD vs. time, see Figure S5 as an example for calculating Li diffusion coefficient.

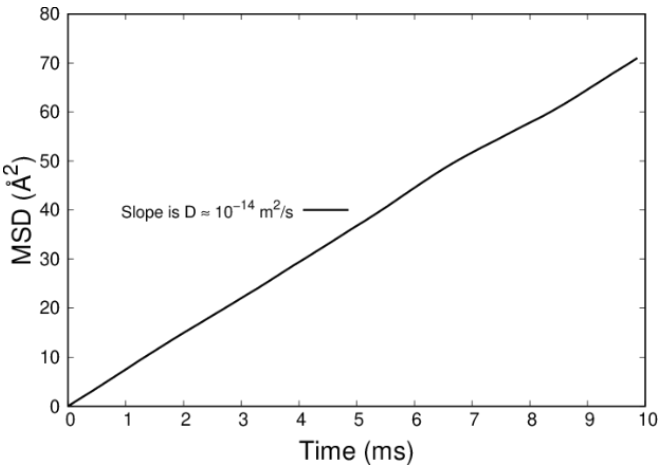

Figure S5: MSD vs. time

This procedure can be used to validate the link between the introduced diffusion rate constant and the expected diffusion coefficient in the kMC simulation. It is important to mention that in a complex mixture of species the "effective" diffusion constant of specie will be the consequence of the combination of all possible diffusive events encountered for this specie. The example given in Figure S5 only allows validating in the kMC setup the appropriate link between the average distance between sites, the diffusive rate constant and the expected diffusion coefficient in a homogeneous media.

2.2 Parameters used in the kMC simulation and box size

Table S3: Parameters used in the kMC simulation: list of reactions, energy barriers for the forward reaction E_b (kJ/mol), backward reaction E_{bb} (kJ/mol) from our DFT calculations, and diffusion coefficient D (m^2s^{-1})

	EC Decomposition Reactions in kMC	in isolation		over Li_2CO_3 (001)		over Li_2O (111)	
		E_b	**E_{bb}**	**E_b**	**E_{bb}**	**E_b**	**E_{bb}**
R0	Li^0 + EC → cLi-EC•	0	63	0	213	0	238
RI	cLi-EC• → oLi-EC•	23	118	53	150	42	126
RII	oLi-EC• → $LiCO_3$• + C_2H_4	65	2	62	34	48	65
RIII	Li^0 + oLi-EC• → Li_2CO_3 + C_2H_4	0	375	0	362	0	356
RIV	oLi-EC• + oLi-EC• → Li_2BDC	0	383	13	374	53	418
RV	oLi-EC• + $LiCO_3$• → Li_2EDC + C_2H_4	0	322	0	232	0	224
RVI	Li^0 + $LiCO_3$• → Li_2CO_3	0	437	0	391	0	339
	Li^0 Diffusion	$D_{Li\_Li_2CO_3} \approx 10^{-14}$ m^2s^-		$D_{Li\_Li_2O} \approx 10^{-16}$ m^2s^-			
	EC Diffusion	$D_{EC\_bulk} \approx 10^{-10}$ m^2s^{-1}		$D_{EC\_SEI} \approx 10^{-13}$ m^2s^{-1}			

Simulation Box

Figure S6: Simulation box size: 8.8 nm × 8.8 nm × 35.2. the lower green box compartment represents Li-metal, and the upper compartment represents the bulk EC

2.3 kMC Results

2.3.1 Effect of Initial Number of Layers of Li_2CO_3

The concentration profile of species (e.g., Li_2BDC) with time is almost the same and is independent of the initial number of Li_2CO_3 layers, see Figure S7. The only expected difference is the final concentration of Li_2CO_3 in the case where we start with 8 layers since we start the simulation with more Li_2CO_3 species to form the initial 8 layers of Li_2CO_3 compared to the case when only 2 layers are used

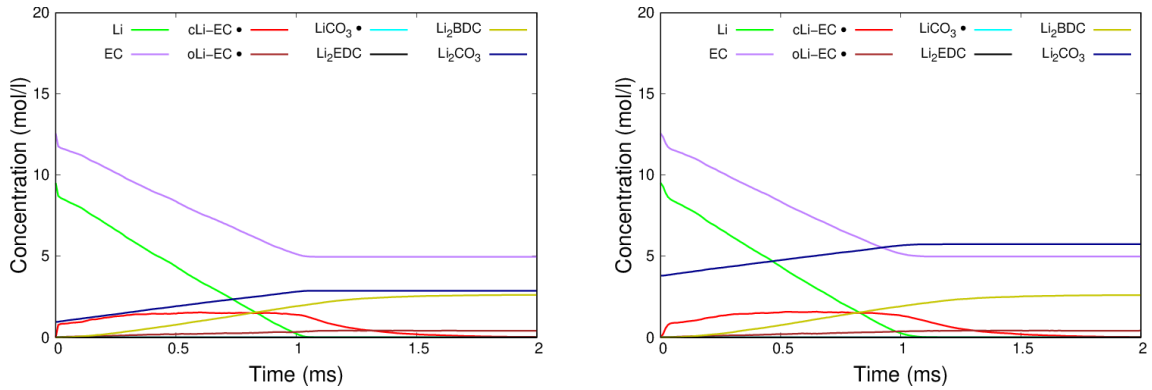

Figure S7: Concentration of species vs. time for EC decomposition reactions over for 2 (left) and 8 (right) initial preformed layers of Li_2CO_3 (001)

2.3.2 Effect of Polymeric Environment in the Organic Part of the SEI

The initial condition and concentration profile vs. time for EC decomposition reaction over 4 initial preformed layers of Li_2CO_3 (001) assuming a strong slowing down of the mobility of the product species can be observed in Figure S8a and S8b respectively. The concentration profile of species and the linear loss of Li^0 is almost the same as when the organic products move, see Figure 4 (e-h). We only noticed a small increase in the final concentration of the inorganic species and a shorter final thickness of the organic layer, see Figure S8c, S8e and Figure S9.

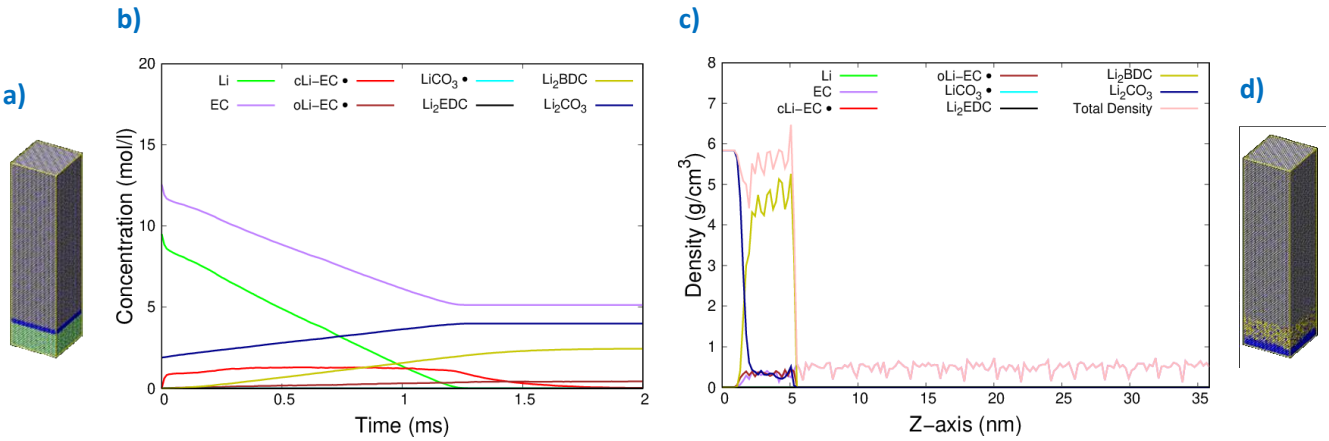

Figure S8: a-d) EC decomposition reactions over 4 initial preformed layers of Li_2CO_3 (001) assuming a strong slowing down of the mobility of the products (polymeric environment) : a) Initial conditions b) Variation of the concentration of species vs. time c) Specific mass density profile along the Z-axis of the simulation box d) Snapshots of the simulation box after 1.5 ms.

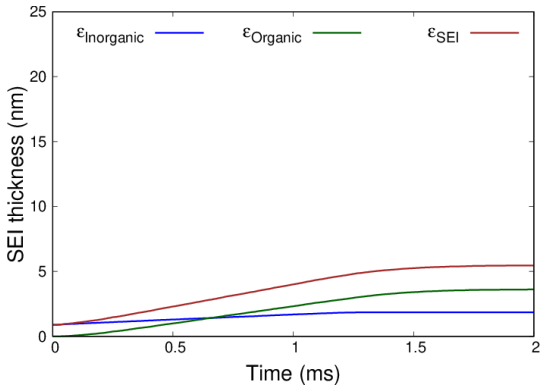

Figure S9: SEI growth for EC decomposition reaction over 4 initial preformed layers of Li_2CO_3 (001) assuming a strong slowing down of the mobility of the product species

2.3.3 EC Decomposition Reactions over Li_2O (111)

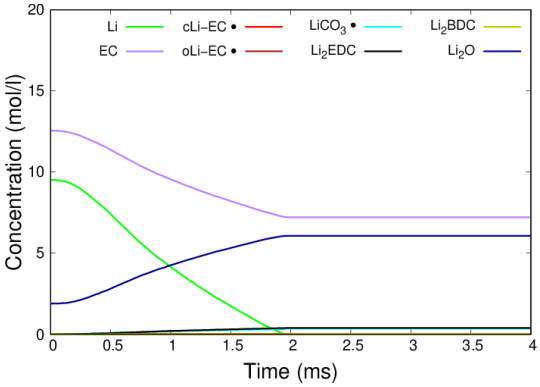

Figure S10: Concentration of species vs. time for EC decomposition reactions over 4 initial preformed layers of Li_2O (111)

2.3.4 EC Decomposition Reactions in the Gas-Phase in Isolation over 4 initial Preformed Layers of Li_2CO_3

To check weather carrying reactions over Li_2CO_3(001) is responsible for the linear behavior, we tested the same setup in Figure 4e but using EC decomposition reactions in isolation. We notice the same non-linear behavior as in Figure 4e in isolation but even a lower concentration of organic species Li_2BDC, see Figure S11. It should be noted that we also observe a shift in the time scale from micro to milliseconds since the diffusion of species was reduced to mimic SEI environment.

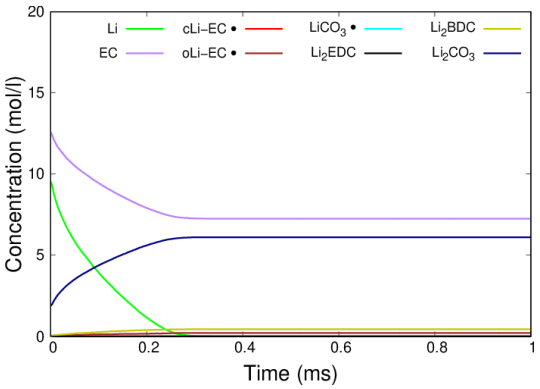

Figure S11: Concentration of species vs. time using EC decomposition reactions in the gas phase in isolation over 4 initial preformed layers of Li_2CO_3

2.3.5 Initial and Final Concentration

Table S4: Initial and final concentration of all species for Figures 4b,4f and S9

		Li	EC	cLi-EC•	oLi-EC•	$LiCO_3$•	C_2H_4	CO_2	Li_2CO_3	Li_2O	Li_2BDC	Li_2EDC
In Isolation	Initial	9.7	12.8	0.0	0.0	0.0	0.0	0.0	0.0	0.0	0.0	0.0
	Final	0.0	7.2	0.0	0.16	0.0	4.2	0.0	4.2	0.0	0.6	0.0
Li_2CO_3 (001)	Initial	9.5	12.6	0.0	0.0	0.0	0.0	0.0	1.9	0.0	0.0	0.0
	Final	0.0	5.0	0.0	0.4	0.0	1.9	0.0	3.8	0.0	2.6	0.0
Li_2O (111)	Initial	9.5	12.6	0.0	0.0	0.0	0.0	0.0	0.0	1.9	0.0	0.0
	Final	0.0	7.2	0.0	0.0	0.4	5.0	3.7	0.0	6.1	0.01	0.4

2.3.6 Intermediate Snapshot for Reactions over Li_2CO_3 (001)

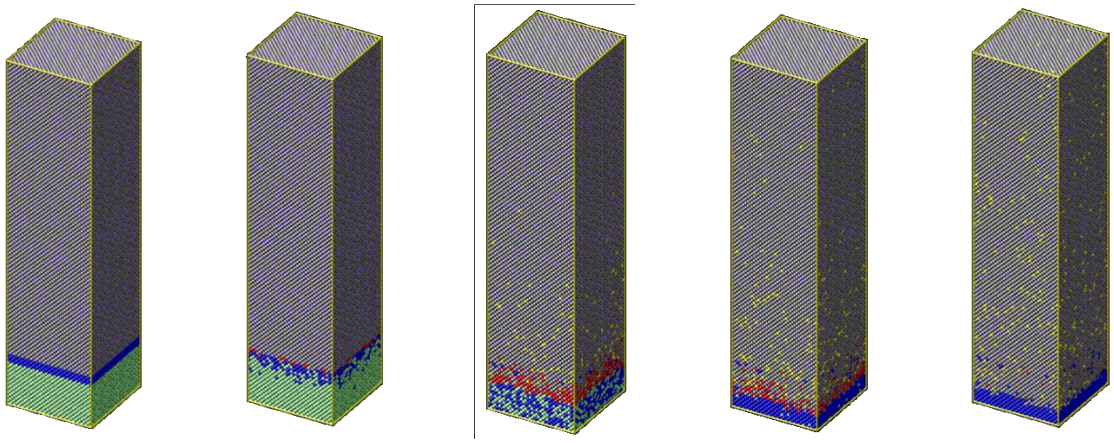

0 0.005 ms 0.6 ms 1 ms 1.2 ms

Figure S12: Intermediate Snapshot for Reactions over Li_2CO_3 (001), the colors are represented in Figure 4.

2.3.7 Effect of a larger Box Size:

We have used a larger box size (17.6 nm × 17.6 nm× 70.4 nm) to see an eventual system-size effect behavior in our simulation results. We notice no significative effect of using a larger simulation box on the concentration profile of species with time, as can be seen in Figure S13.

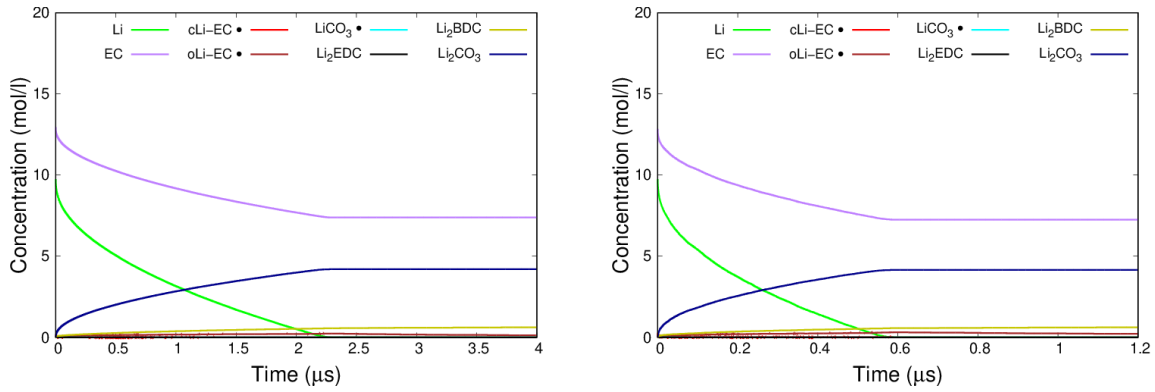

17.6 nm × 17.6 nm × 70.4 nm 8.8 nm × 8.8 nm × 35.2 nm

Figure S13: Concentration of species vs. time and density profile for EC decomposition reactions in the gas phase in isolation using different simulation box size

2.3.8 Effect of Seeds Used to Run kMC Simulations

We notice no effect of the number used as initial seed to run the kMC simulation on the concentration profile of species with time, see Figure S14.

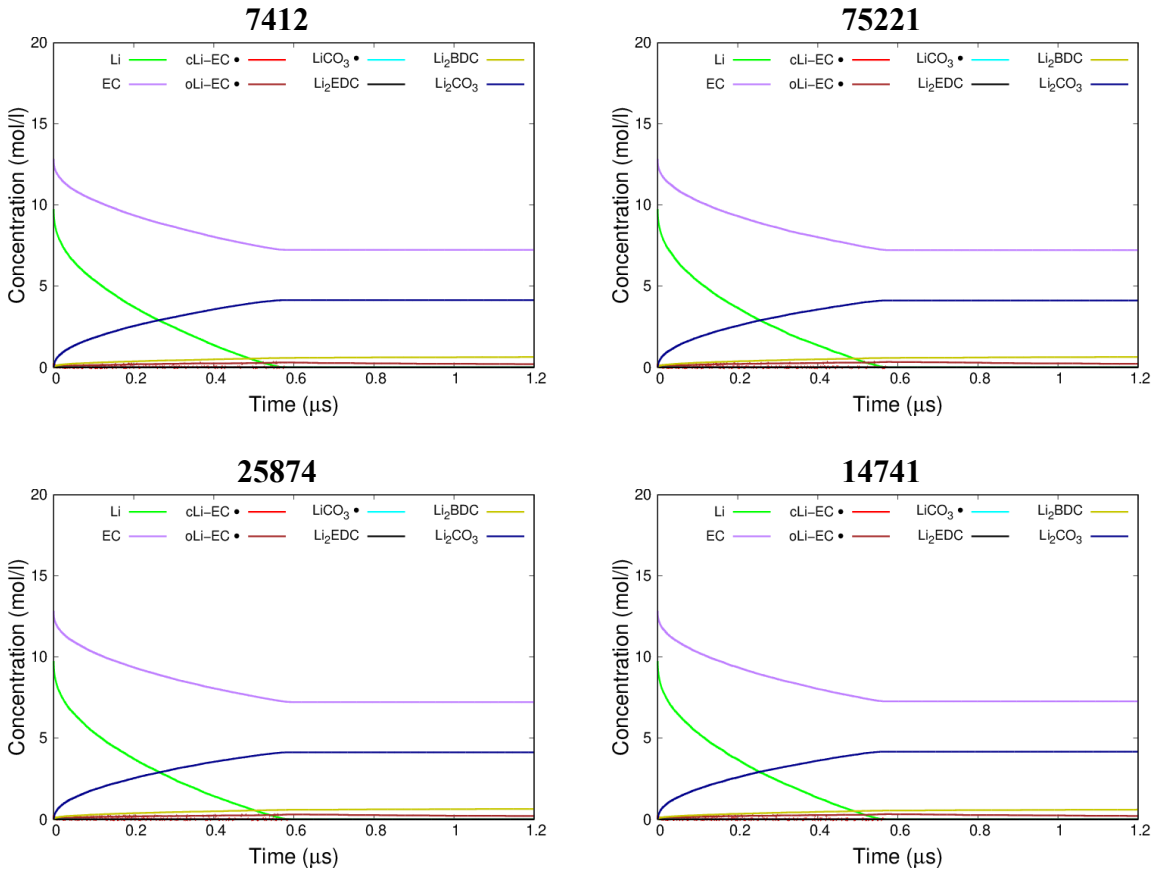

Figure S14: Concentration of species vs. time and density profile for EC decomposition reactions in the gas phase in isolation using different initial seeds numbers.

2.3.9 Effect of Number of Cores Used

We notice no effect of the number of cores used on the concentration profile of species with time, as can be seen in Figure S15.

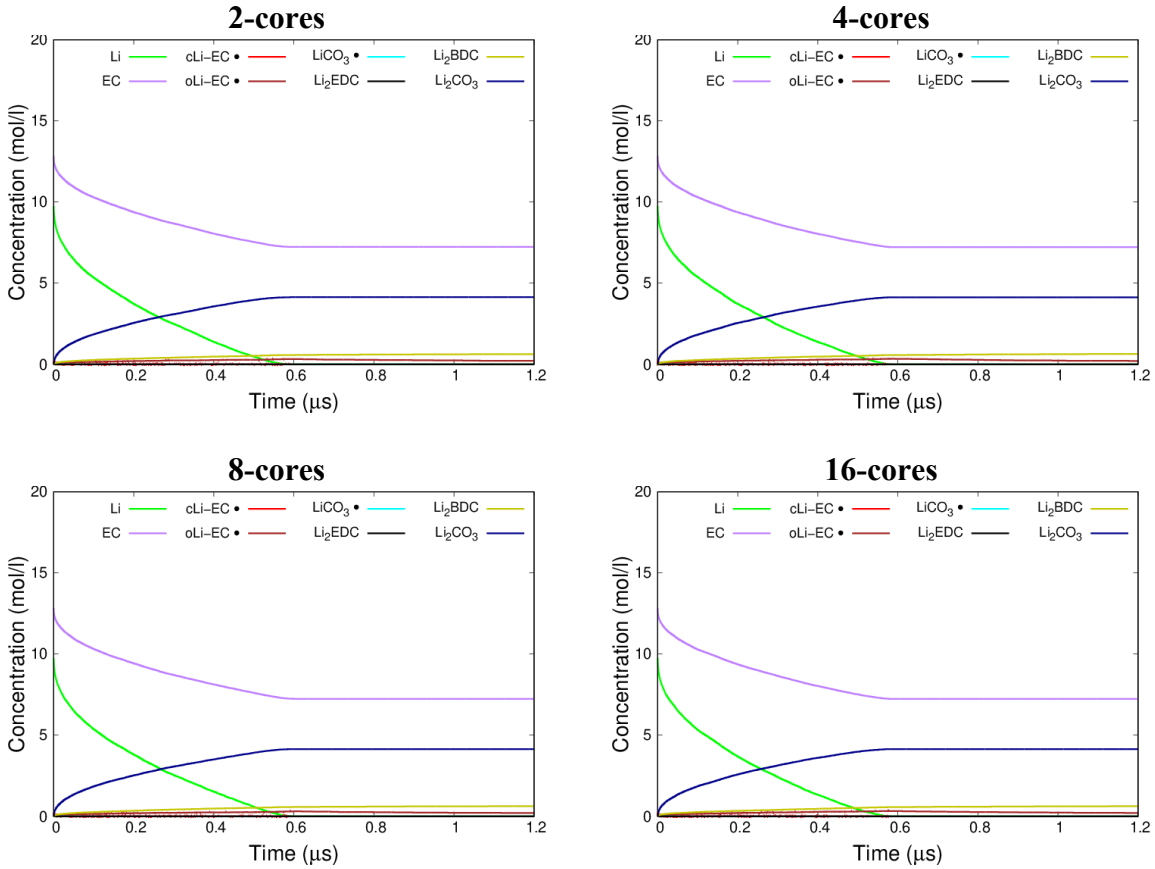

Figure S15: Concentration of species vs. time and density profile for EC decomposition reactions in the gas phase in isolation using different CPU cores

2.4 SPPARKS's Input File and Code Modification

2.4.1 Typical Input file for SPPARKS: EC decomposition reactions in isolation

For a practical point of view, to specify an event in SPPARKS, if two species are meant to react to form a new species, a vacant site would be added to conserve number of sites. We also need to identify number of sites involved in any event and provide the type of sites (e.g., fcc), the name of the species involved and the energy barrier, see Figure S16.

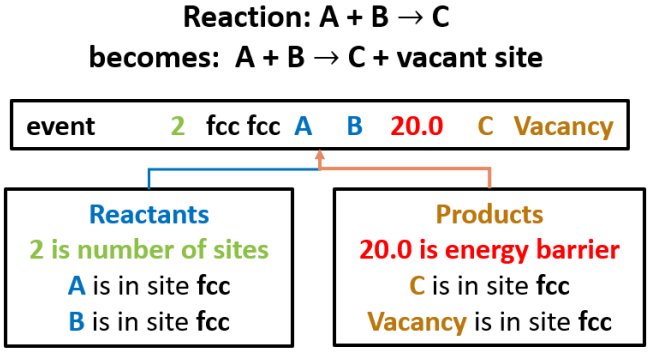

Figure S16: Specifying events in SPPARKS software

Table S5 shows the names used for the species in SPPARKS.

Table S5: The names used for the species in SPPARKS code

Species	Li	EC	oLi-EC•	$LiCO_3$•	cLi-EC•	Li_2EDC	Li_2BDC	Li_2CO_3	vacant site
In SPPARKS	li	ec	oec	carb	eth	liedc	libdc	carbonate	vac

 # Example of SPPARKS Input file (modified Erbium application)

```
seed          9999
app_style     erbium

lattice       fcc 4.4 #cereate FCC lattice
region        box block 0 20 0 20 0 80
boundary      p p n #periodicity in x and y only
create_box    box
create_sites  box value i1 0 basis 1*4 1 # basis 5*8 2 basis 9* 3 #cereate sites in FCC lattice
read_sites    SS_4.4_n_layers_0 # read initial configuration
sector        yes
solve_style   tree
```

```
##############REACTIONS EVENTS

event        1 fcc eth 1098938320.18 oec
event        1 fcc oec 0.0000000310  eth
event        1 fcc oec 42.04041642  carb
event        1 fcc carb 4460867100119 oec
event        2 fcc fcc ec li -74 eth vac
event        2 fcc fcc ec li -74 vac eth
event        2 fcc fcc eth vac -11 ec li
event        2 fcc fcc vac eth -11 ec li
event        2 fcc fcc oec carb -74 vac liedc
event        2 fcc fcc oec carb -74 liedc vac
event        2 fcc fcc vac liedc 248 oec carb
event        2 fcc fcc liedc vac 248 oec carb
event        2 fcc fcc oec oec -74 vac libdc
event        2 fcc fcc vac libdc 309 oec oec
event        2 fcc fcc li carb -74 vac carbonate
event        2 fcc fcc li carb -74 carbonate vac
event        2 fcc fcc vac carbonate 363 li carb
event        2 fcc fcc carbonate vac 363 li carb
event        2 fcc fcc li oec -74 vac carbonate
event        2 fcc fcc li oec -74 carbonate vac
event        2 fcc fcc vac carbonate 301 li oec
event        2 fcc fcc carbonate vac 301 li oec
##############DIFFUSION EVENTS (the values below when inserted in SPPARKS gives us
the diffusion coefficient needed for Li and EC diffusion).
event        2 fcc fcc eth ec -38 ec eth
event        2 fcc fcc oec ec -38 ec oec
event        2 fcc fcc li carbonate -32 carbonate li
event        2 fcc fcc vac ec -55 ec vac
event        2 fcc fcc liedc ec -38 ec liedc
event        2 fcc fcc libdc ec -38 ec libdc
event        2 fcc fcc carb ec -38 ec carb
##############TEMPERATURE IN UNITS OF R*T, where R is universal gas constant
(0.008314 kJ/ (mol* K)) and T is Temperature (298)
temperature     2.48
#### Output file customization
diag_style      erbium stats yes &
            list li ec oec carb eth liedc libdc carbonate inner vac events  s1 s2 s3 s4 d1 d2 d3
d4 d5 d6 d7 d8 d9  d10 d11  d12 d13 d14 d15 d16 d17 d18 d19 d20 d21 d22 d23 d24 d25
stats         0.0000000001
dump myDump image 0.0000001  dump.*.ppm i2 site crange 1 100 drange lo hi sdiam 3.5
size 1024 1024
dump_modify  myDump scolor *
lightgreen/mediumpurple/brown/cyan/red/black/yellow/blue/white/gray  #cwrap  yes
#scolor * red/white/black backcolor gray
dump          2 sites 1 my.sites.* id i1 i2  z
```

```
dump          1 text 0.000001 dump.erbium  i2 z
#############SIMULATION TIME
run           0.000002
```

2.4.2 Code Modification of Erbium application (SPPARKS)

There erbium application has two files: app_erbium.cpp for the calculations and diag_erbium.cpp for the output. Initially, the app_erbium.cpp code has four species erbium (er), hydrogen (h), helium (he), and vacancy (vac). We changed the names of er, h and he to li (Li), ec (EC), and oec (cLi-EC•), respectively. We added more species to adapt the code to our SEI model: carb ($LiCO_3$•), eth (cLi-EC•), liedc (Li_2EDC), libdc (Li_2BDC), carbonate (Li_2CO_3) and inner (extra species, we did not use it). Table S6 shows the original app_erbium.cpp code and our major modifications. The file "diag_erbium.cpp" was also modified to be adapted to the modified app_erbium.cpp, see Table S7.

Table S6: SPPARKS code major modifications (app_erbium.cpp)

Original Code

```
enum{ZERO,ERBIUM,HYDROGEN,HELIUM,VACANCY};

if (strcmp(arg[2],"er") == 0) sinput[none] = ERBIUM;
else if (strcmp(arg[2],"h") == 0) sinput[none] = HYDROGEN;
else if (strcmp(arg[2],"he") == 0) sinput[none] = HELIUM;
if (type[i] == FCC) return proball = 0.0;
```

Major Modifications

```
enum{ZERO,ERBIUM,HYDROGEN,HELIUM,CARB,ETH,PLIEDC,PLIBDC,CARBONATE,INNER,VA
CANCY};
if (strcmp(arg[2],"li") == 0) sinput[none] = ERBIUM;
else if (strcmp(arg[2],"ec") == 0) sinput[none] = HYDROGEN;
else if (strcmp(arg[2],"oec") == 0) sinput[none] = HELIUM;
else if (strcmp(arg[2],"carb") == 0) sinput[none] = CARB;
else if (strcmp(arg[2],"eth") == 0) sinput[none] = ETH;
else if (strcmp(arg[2],"liedc") == 0) sinput[none] = PLIEDC;
else if (strcmp(arg[2],"libdc") == 0) sinput[none] = PLIBDC;
else if (strcmp(arg[2],"carbonate") == 0) sinput[none] = CARBONATE;
else if (strcmp(arg[2],"inner") == 0) sinput[none] = INNER;
// if (type[i] == FCC) return proball = 0.0;  ( to allow FCC event to occur)
```

Table S7: SPPARKS code major modifications (diag_erbium.cpp)

Original Code

```
enum{ZERO,ERBIUM,HYDROGEN,HELIUM,VACANCY};
enum{ER,H,HE,VAC,EVENTS,ONE,TWO,THREE};
if (strcmp(list[i],"er") == 0) which[i] = ER;
else if (strcmp(list[i],"h") == 0) which[i] = H;
else if (strcmp(list[i],"he") == 0) which[i] = HE;
if (which[i] == ER || which[i] == H || which[i] == HE || which[i] == VAC)
int sites[5],ivalue;
sites[ERBIUM] = sites[HYDROGEN] = sites[HELIUM] = sites[VACANCY] = 0;
if (which[i] == ER) ivalue = sites[ERBIUM];
else if (which[i] == H) ivalue = sites[HYDROGEN];
else if (which[i] == HE) ivalue = sites[HELIUM];
```

Major Modifications

```
enum{ZERO,ERBIUM,HYDROGEN,HELIUM,CARB,ETH,PLIEDC,PLIBDC,CARBONATE,INNER,
VACANCY};
enum{LI,EC,OEC,CARBO,ETHE,LIEDC,LIBDC,CARBON,INN,VAC,EVENTS,ONE,TWO,THREE};
if (strcmp(list[i],"li") == 0) which[i] = LI;
else if (strcmp(list[i],"ec") == 0) which[i] = EC;
else if (strcmp(list[i],"oec") == 0) which[i] = OEC;
else if (strcmp(list[i],"carb") == 0) which[i] = CARBO;
else if (strcmp(list[i],"eth") == 0) which[i] = ETHE;
else if (strcmp(list[i],"liedc") == 0) which[i] = LIEDC;
else if (strcmp(list[i],"libdc") == 0) which[i] = LIBDC;
else if (strcmp(list[i],"carbonate") == 0) which[i] = CARBON;
else if (strcmp(list[i],"inner") == 0) which[i] = INN;
if (which[i] == LI || which[i] == EC || which[i] == OEC || which[i] == CARBO || which[i] ==
ETHE ||  which[i] == LIEDC || which[i] == LIBDC || which[i] == CARBON || which[i] ==
INN || which[i] == VAC)
int sites[11],ivalue;
sites[ERBIUM] = sites[HYDROGEN] = sites[HELIUM] = sites[CARB] = sites[ETH] =
sites[PLIEDC] = sites[PLIBDC] = sites[CARBONATE] =  sites[INNER] =  sites[VACANCY] = 0;
if (which[i] == LI) ivalue = sites[ERBIUM];
if (which[i] == EC) ivalue = sites[HYDROGEN];
else if (which[i] == OEC) ivalue = sites[HELIUM];
else if (which[i] == CARBO) ivalue = sites[CARB];
else if (which[i] == ETHE) ivalue = sites[ETH];
else if (which[i] == LIEDC) ivalue = sites[PLIEDC];
else if (which[i] == LIBDC) ivalue = sites[PLIBDC];
else if (which[i] == CARBON) ivalue = sites[CARBONATE];
else if (which[i] == INN) ivalue = sites[INNER];
```

REFERENCES

(1) Jansen, A. P. J. An Introduction To Monte Carlo Simulations Of Surface Reactions. *arXiv: Statistical Mechanics* **2003**. https://doi.org/10.1007/978-3-642-29488-4

(2) Chorkendorff, I.; Niemantsverdriet, J. W. *Concepts of modern catalysis and kinetics*; Wiley-VCH, **2003**. https://doi.org/10.1002/3527602658

(3) Ramasubramanian, A.; Yurkiv, V.; Foroozan, T.; Ragone, M.; Shahbazian-Yassar, R.; Mashayek, F. Lithium Diffusion Mechanism through Solid–Electrolyte Interphase in Rechargeable Lithium Batteries. *J. Phys. Chem. C* **2019**, *123* (16), 10237–10245. https://doi.org/10.1021/acs.jpcc.9b00436

(4) Salciccioli, M.; Stamatakis, M.; Caratzoulas, S.; Vlachos, D. G. A review of multiscale modeling of metal-catalyzed reactions: Mechanism development for complexity and emergent behavior. *Chem. Eng. Sci.* **2011**, *66* (19), 4319–4355. https://doi.org/10.1016/j.ces.2011.05.050

(5) Bortz, A.B.; Kalos, M.H.; Lebowitz, J.L.. A new algorithm for Monte Carlo simulation of Ising spin systems. J. Comput. Phys. 1975, 17 (1), 10–18. https://doi.org/10.1016/0021-9991(75)90060-1

(6) Voter, A. Introduction to the Kinetic Monte Carlo Method. In Radiation Effects in Solids; Sickafus, K. E., Kotomin, E. A., Uberuaga, B. P., Eds.; Springer Netherlands: Dordrecht, **2007**; pp 1−23. https://doi.org/10.1007/978-1-4020-5295-8_1

(7) Corbett C. Battaile. The Kinetic Monte Carlo method: Foundation, implementation, and application. *Comput. Methods Appl. Mech. Eng.* **2008**, *197* (41), 3386–3398. https://doi.org/10.1016/j.cma.2008.03.010